Gauge ambiguities in $(\vec{e},e'\vec{N})$ reactions

James J. Kelly
Department of Physics, University of Maryland, College Park, Maryland 20742
(Received 4 June 1997)

We examine the sensitivity of the distorted-wave impulse approximation for single-nucleon electromagnetic knockout from valence orbitals to ambiguities in the one-body current operator. Violations of current conservation are classified as gauge ambiguities, whereas the elements of a particular class of structural differences off shell are labeled Gordon ambiguities. Gauge ambiguities in differential cross sections and longitudinal response functions are found to increase with missing momentum and to become particularly severe for low-Q^2 kinematical conditions that are far from quasifree but are sometimes used to investigate correlations. The azimuthal asymmetry may provide a useful experimental means for selecting a gauge. Gordon ambiguities increase with Q^2 and are larger for relativistic than for nonrelativistic approaches. Because ambiguities in the one-body current are at least as large as effects due to correlations and there are additional uncertainties due to two-body currents, final-state interactions, and relativistic distortion, we conclude that is unlikely that information about correlations can be extracted from single-nucleon knockout from valence orbitals at large missing momentum. On the other hand, gauge and Gordon ambiguities and uncertainties in final-state interactions have very little effect upon the helicity-dependent recoil polarization, which can be used to investigate the roles of two-body currents and/or possible medium modifications of the one-body current. [S0556-2813(97)04411-7]

PACS number(s): 25.30.Dh, 24.10.Ht, 24.70.+s, 27.20.+n

I. INTRODUCTION

The $A(e,e'N)B$ reaction provides the most direct experimental probe of momentum distributions in nuclei that is presently available. The $(e,e'p)$ reaction has been used extensively to determine missing momentum distributions and spectroscopic factors for valence hole states in many nuclei; recent reviews of this subject may be found in Refs. [1–5]. The plane-wave impulse approximation (PWIA) provides a physically appealing, albeit simplistic, model of this reaction in which a nucleon with initial momentum $\mathbf{p}_m=\mathbf{p}'-\mathbf{q}$ absorbs a virtual photon $(\omega,\mathbf{q})$ and emerges with final momentum $(E',\mathbf{p}')$. The differential cross section

$$\text{PWIA}\Rightarrow\frac{d\sigma}{d\varepsilon_f d\Omega_e d\varepsilon_N d\Omega_N}=K\sigma_{eN}S(\mathbf{p}_m,E_m) \qquad (1)$$

can then be represented by the product of an elementary cross section σ_{eN}, a phase-space factor K, and the probability, $S(\mathbf{p}_m,E_m)$, that removal of a nucleon with momentum $\mathbf{p}_m$ will result in a final state of the residual system with missing energy $E_m=m_N+m_B-m_A$. Thus, to the extent that this simple picture applies, the knockout cross section is proportional to the single-nucleon spectral function for the target, which then forms a bridge between the experiment and the theory of nuclear structure. However, the spectral function is not itself an experimental observable, but rather must be deduced from cross section measurements using a suitable reaction model. Therefore, to cross this bridge we must refine the picture to account for electron distortion, final-state interactions, modifications of the electromagnetic vertex function for bound particles, and meson-exchange and isobar currents.

Corrections to this simple picture due to initial- and final-state interactions are usually evaluated using the distorted-wave impulse approximation (DWIA) in which electron wave functions are distorted by Coulomb potentials and the ejectile wave function is distorted by an optical potential that also accounts for the flux that is diverted by final-state interactions into more complicated channels. For modest missing momenta one generally finds that the fitted momentum distributions are almost independent of the kinematics of the reaction, which supports the applicability of the distorted-wave approximation under those conditions [1–5].

A consistent theoretical description of the single-hole spectral functions for both nuclear matter and finite nuclei has emerged from a vast body of work employing diverse methods. A brief review of this work and an extensive set of references may be found in Ref. [1]. For nuclear matter, short-range and tensor correlations deplete the Fermi sphere by approximately 15–20% and populate nominally empty orbitals, thereby producing a long tail on the momentum distribution. The quasihole strength near the Fermi surface is then about 0.5–0.7 and increases with binding energy. In finite nuclei, coupling to low-lying surface modes (long-range correlations) produces additional depletion of the valence hole states, increases the population of nominally empty orbitals, and spreads the quasihole strength over several fragments. The calculated missing momentum distributions for valence-hole states generally follow mean-field predictions (Hartree-Fock) quite closely in shape, differing mainly by overall spectroscopic factors. Thus, the momentum distribution for $p_m\lesssim 250$ MeV/c is dominated by low-lying quasihole contributions, but as the missing momentum increases more complicated continuum configurations at high excitation energy dominate. Short-range and tensor correlations spread the high momentum strength over several hundred MeV of excitation energy. For example, a partial-wave analysis of the hole spectral function for ^{16}O by Polls *et al.* [6] shows dramatic enhancement at high momenta for

large missing energy while valence states continue to follow mean-field momentum distributions rather closely.

Several models suggest that coupling to low-lying surface modes may substantially enhance the missing momentum distributions for quasihole states beyond $p_m > 300$ MeV/c also. For example, the quasiparticle Hamiltonian model of Ma and Wambach [7,8] represents this coupling by a surface-peaked contribution to the effective mass which has the effect of substantially increasing the single-nucleon overlap function for large momenta. Alternatively, the dispersive optical model of Mahaux and co-workers [9–11] relates the surface-peaked feature of the effective mass to the energy dependence of dispersive contributions to the single-particle potential. Bobeldijk *et al.* [12] measured ^{208}Pb$(e,e'p)$ for $300 < p_m < 500$ MeV/c with $(\omega,q) = (110\ \text{MeV}, 221\ \text{MeV}/c)$ and $T_p = 100$ MeV and for low-lying states found significant enhancements with respect to Hartree-Fock wave functions at large momenta. Better agreement with these data was obtained from calculations that applied effective mass corrections of the type suggested by these models of long-range correlations. However, with a value for the Bjorken scaling variable, $x = Q^2/2m\omega$, of only about $x \approx 0.18$, where $x = 1$ corresponds to quasifree kinematics, one must be concerned with the validity of the impulse approximation for these experimental conditions. Furthermore, comparable effects are attributed by van der Sluys *et al.* [13] to two-body currents and by Udías *et al.* [14] to variations of the one-body current operator in a relativistic DWIA.

Saha *et al.* [15] have proposed to measure ^{16}O$(e,e'p)^{15}$N at large missing momentum using quasifree kinematics with $\omega = 0.445$ GeV, $q = 1.0$ GeV/c such that $Q^2 = 0.8$ (GeV/c)^2 and $x = 0.96$. Similarly, Glashausser *et al.* [16] have proposed to measure recoil polarization for modest missing momentum using the same reaction and similar kinematics. The relatively high ejectile energy should help to minimize ambiguities due to final-state interactions while the use of quasifree kinematics is intended to simplify the reaction mechanism. Furthermore, both initial-state and final-state distortions are less important for this relatively light target than for lead. Therefore, it is of considerable interest to investigate the implications of ambiguities in the one-body current operator for these proposed experiments. In addition, we consider the lower-energy ^{16}O$(e,e'p)^{15}$N experiment performed by Blomqvist *et al.* [17] in which valence states were measured for $p_m \lesssim 675$ MeV/c but with kinematics rather far from quasifree.

In this paper we investigate the consequences of ambiguities in the one-body current operator for nonrelativistic DWIA calculations of $(e,e'N)$ reactions over a wide range of experimental conditions. It has long been recognized that optical model calculations violate gauge invariance because the DWIA does not conserve current (e.g., Refs. [18–20]). Therefore, most calculations of $(e,e'p)$ reactions attempt to restore current conservation using an *ad hoc* prescription. The most common prescription, popularized by de Forest [18], is to replace the longitudinal component of the electromagnetic current for the target by a term proportional to the charge component such that $q \cdot J \rightarrow 0$ for the modified current. However, this prescription is not unique and there exist several equally simple and equally (un)worthy alternatives which would all give equivalent results if the model conserved current but which actually give rather different results under some kinematical conditions. As suggested by Pollock *et al.* [21], each of these prescriptions can be associated with a gauge for which the original nonconserved current gives the same results as the modified current. Furthermore, several prescriptions for off-shell extrapolation of the current operator have been proposed [18,22]. These prescriptions are related by the Gordon identity and are equivalent on shell but violate current conservation off shell and also give different results for the same gauge. Thus, it is useful to distinguish between gauge ambiguities related to violations of current conservation for a particular one-body current operator and Gordon ambiguities related to structural differences which become manifest off shell.

Additional flexibilities in the general structure of the off-shell current operator are not considered here. Naus *et al.* [20] demonstrated that the half off-shell vertex function contains six operators with four independent form factors, each of which depends upon two Lorentz scalars. Therefore, limitation of the vertex function to only two form factors depending upon only a single kinematic variable represents a rather severe truncation which can only be justified on the basis of a theory of the underlying dynamics of the off-shell γN vertex.

Ideally one should evaluate the nuclear electromagnetic current using a many-body Hamiltonian which accurately describes both bound and scattering states. Calculations for ^{16}O$(e,e'N)$ have been performed for $T_N \approx 70-100$ MeV by Ryckebusch *et al.* [23] using a Hartree-Fock (HF) random phase approximation (RPA) model based upon a Skyrme interaction [24]. Both bound and continuum wave functions are generated within the HF mean field for the Skyrme interaction and long-range correlations are described by the RPA. The current operator is also based upon the HF Hamiltonian. Thus, this approach preserves gauge invariance and avoids orthogonality defects which can be important at large p_m. On the other hand, because the mean field is real, attenuation of the scattered flux must be described by explicit coupling to the open channels. Coupling to all single-nucleon emission channels is included within the RPA, but more complicated configurations are omitted. Hence, although this model is internally consistent, its description of the final-state interactions is not adequate. This model is most applicable for small ejectile energies, but as the energy increases final-state interactions involve increasingly complicated configurations, including meson production, which cannot be adequately described by the HF-RPA approach. For high-energy ejectiles there are no practical alternatives to distorted wave or Glauber approaches, neither of which conserve current.

Fortunately, because gauge ambiguities appear to have relatively little practical significance when the missing momentum is relatively small and the kinematics are nearly quasifree [5,1], one is reasonably confident that momentum distributions for $p_m \lesssim 250$ MeV/c can be extracted accurately from quasifree $(e,e'p)$ data using DWIA analyses. However, recently there have been several experiments performed or proposed that are intended to investigate correlations using single-nucleon knockout at large missing momenta [12,17,15], but because the kinematics of such experiments are often rather far from quasifree it becomes

necessary to reexamine the consequences of various ambiguities in the reaction mechanism. In addition, there are proposed experiments [16] designed to investigate medium modifications of the nucleon electromagnetic current using recoil polarization. Although there are additional ambiguities due to the off-shell extrapolation of the current operator for bound nucleons or from the choice of optical potential, in this paper we investigate the consequences of gauge and Gordon ambiguities in $(\vec{e},e'\vec{N})$ reactions over a wide range of kinematical conditions.

The model is outlined in Sec. II and calculations for both the Mainz and the TJNAF $^{16}\mathrm{O}(e,e'p)^{15}\mathrm{N}$ experiments are presented in Sec. III. Our conclusions are summarized in Sec. IV.

II. MODEL

A. One-photon-exchange approximation

For semiexclusive $A(e,e'x)B$ reactions in which only a single discrete state or narrow resonance of the target is excited, the one-photon-exchange approximation in the Feynman gauge for the fivefold differential cross section takes the form

$$\frac{d^5\sigma}{d\varepsilon_f d\Omega_e d\Omega_x}=K\frac{\varepsilon_f}{\varepsilon_i}\frac{\alpha^2}{Q^4}\eta_{\mu\nu}\mathcal{W}^{\mu\nu}, \tag{2}$$

where

$$K=\mathcal{R}\frac{p_x\varepsilon_x}{(2\pi)^3} \tag{3}$$

is a phase-space factor, $k_i=(\varepsilon_i,\mathbf{k}_i)$ and $k_f=(\varepsilon_f,\mathbf{k}_f)$ are the initial and final electron momenta, $p_A=(\varepsilon_A,\mathbf{p}_A)$ and $p_B=(\varepsilon_B,\mathbf{p}_B)$ are the initial and final target momenta, $p_x=(\varepsilon_x,\mathbf{p}_x)$ is the ejectile momentum, $q=k_i-k_f=(\omega,\mathbf{q})$ is the momentum transfer carried by the virtual photon, $Q^2=-q_\mu q^\mu=\mathbf{q}^2-\omega^2$ is the photon virtuality, and

$$\mathcal{R}=\left|1-\frac{\varepsilon_x}{\varepsilon_B}\frac{\mathbf{p}_x\cdot\mathbf{p}_B}{\mathbf{p}_x\cdot\mathbf{p}_x}\right|^{-1} \tag{4}$$

is a recoil factor which adjusts the nuclear phase space [25] for the constraint on missing energy. In the extreme relativistic limit, only the longitudinal component of the electron polarization is relevant and the electron response tensor [26]

$$\eta_{\mu\nu}=\frac{1}{2}[\eta^u_{\mu\nu}+h\eta^h_{\mu\nu}] \tag{5}$$

can be separated into helicity-independent, $\eta^u_{\mu\nu}$, and helicity-dependent, $\eta^h_{\mu\nu}$, contributions of the form

$$\eta^u_{\mu\nu}=K_\mu K_\nu-q_\mu q_\nu-Q^2 g_{\mu\nu}, \tag{6a}$$

$$\eta^h_{\mu\nu}=-i\varepsilon_{\mu\nu\alpha\beta}q_i^\alpha K_f^\beta, \tag{6b}$$

where $\varepsilon_{\mu\nu\alpha\beta}$ is the completely antisymmetric tensor and $K=k_i+k_f$.

Similarly, one defines the unpolarized nuclear response tensor as

$$\mathcal{W}_{\mu\nu}=\langle J_\mu J_\nu^\dagger\rangle, \tag{7}$$

where the angular brackets denote products of matrix elements appropriately averaged over initial states and summed over final states. Recoil polarization is included via the generalization

$$\mathcal{W}_{\mu\nu}(\hat{\boldsymbol{a}})=\langle J_\mu J_\nu^\dagger\boldsymbol{\sigma}\cdot\hat{\boldsymbol{a}}\rangle, \tag{8}$$

where $\hat{\boldsymbol{a}}$ is desired nucleon polarization component and where the Pauli matrix refers to the ejectile spin. Conservation of the nuclear electromagnetic current requires

$$q_\mu J^\mu=0\Rightarrow q_\mu\mathcal{W}^{\mu\nu}=\mathcal{W}^{\mu\nu}q_\nu=0,$$

but this principle is usually violated when approximations are made to the complicated nuclear dynamics.

B. Relationship between gauge and prescription for current conservation

Most recent calculations attempt to restore current conservation by modifying the longitudinal component of the nuclear current using the *ad hoc* replacement

$$J_q\rightarrow\frac{\omega}{q}J_0. \tag{9}$$

This procedure was originally applied to $(e,e'p)$ calculations by de Forest [27,18] and was justified by the argument that the charge operator was understood better than the longitudinal convection current. However, we do not find this argument compelling and note that there exist several alternative prescriptions which are equally simple to apply and which are equivalent in principle. As suggested by Pollock *et al.* [21], it is useful to associate the prescription for restoration of current conservation with the gauge that gives the same results without modifying the current. Thus, the de Forest prescription is associated with the Coulomb gauge. Similarly, the prescription

$$J_0\rightarrow\frac{q}{\omega}J_q \tag{10}$$

is associated with the Weyl gauge. Finally, the prescription

$$J_\mu\rightarrow J_\mu+\frac{J\cdot q}{Q^2}q_\mu \tag{11}$$

is associated with the Landau gauge and has been used by Mougey *et al.* [28]. However, it is important to recognize that although the current associated with the Landau gauge is conserved, the piece that restores current conservation does not actually affect the observables because it is orthogonal to the electron tensor. Therefore, calculations using a conserved current obtained via the Landau prescription are equivalent to using the original nonconserved current in the Feynman gauge.

C. Current operator

Matrix elements of the nucleon electromagnetic current can be expressed in the form

$$\langle p_f s_f|J^\mu|p_i s_i\rangle=\overline{u_f}\Gamma^\mu(p_f,p_i)u_i, \tag{12}$$

where Γ^μ is the electromagnetic vertex function for the nucleon and where the spinors are denoted by u_i and u_f. For a free nucleon, the electromagnetic vertex function can be expressed in several equivalent forms [22]

$$\Gamma_1^\mu=\gamma^\mu G_M(Q^2)-\frac{P^\mu}{2m}\kappa F_2(Q^2), \tag{13a}$$

$$\Gamma_2^\mu=\gamma^\mu F_1(Q^2)+i\sigma^{\mu\nu}\frac{q_\nu}{2m}\kappa F_2(Q^2), \tag{13b}$$

$$\Gamma_3^\mu=\frac{P^\mu}{2m}F_1(Q^2)+i\sigma^{\mu\nu}\frac{q_\nu}{2m}G_M(Q^2), \tag{13c}$$

where F_1 is the Dirac form factor, F_2 is the Pauli form factor, and κ is the anomalous part of the magnetic moment. The Sachs electric and magnetic form factors [29] are $G_E=F_1-\tau\kappa F_2$ and $G_M=F_1+\kappa F_2$, where $\tau=Q^2/4m^2$. Additional variations can be obtained from linear combinations. These forms are related by the Gordon identity [30,31] and give identical results for a free nucleon but differ when the kinematics for a bound nucleon are taken off shell. The de Forest prescription for extrapolation of these operators off shell employs free spinors for momentum $\mathbf{p}$ and mass m, but replaces the energy E used within the vertex function by the value $\overline{E}$ it would have had if the nucleon were on shell in the initial state. Thus, the off-shell extrapolation is obtained by replacing the energy transfer and the momenta by

$$q=(\omega,\mathbf{q})\rightarrow\overline{q}=(\overline{\omega},\mathbf{q}),$$

$$P=p'+p\rightarrow\overline{P}=(E'+\overline{E},\mathbf{p}'+\mathbf{p}),$$

in the nucleon current operator. However, the form factors are still evaluated at the asymptotic momentum transfer, Q^2 rather than $\overline{Q^2}$. Therefore, we obtain the alternative prescriptions

$$\overline{\Gamma_1^\mu}=\gamma^\mu G_M(Q^2)-\frac{\overline{P^\mu}}{2m}\kappa F_2(Q^2), \tag{14a}$$

$$\overline{\Gamma_2^\mu}=\gamma^\mu F_1(Q^2)+i\sigma^{\mu\nu}\frac{\overline{q_\nu}}{2m}\kappa F_2(Q^2), \tag{14b}$$

$$\overline{\Gamma_3^\mu}=\frac{\overline{P^\mu}}{2m}F_1(Q^2)+i\sigma^{\mu\nu}\frac{\overline{q_\nu}}{2m}G_M(Q^2). \tag{14c}$$

Several other prescriptions for off-shell extrapolation based upon effective mass concepts may be found in Refs. [5, 18].

We describe differences between off-shell vertex functions obtained using the Gordon identity as Gordon ambiguities. The importance of Gordon ambiguities is expected to increase with Q^2 [20]. Furthermore, distortion of nucleon spinors in Dirac mean fields tends to make relativistic models more sensitive to Gordon ambiguities than nonrelativistic DWIA models [22,14].

Unfortunately, because none of these off-shell vertex functions explicitly conserves electromagnetic current, it becomes necessary to restore current conservation in an *ad hoc* manner as described in Sec. II B. Thus, after modification of the current operator, one obtains a family of off-shell vertex functions $\{\overline{\Gamma_{cc1}},\overline{\Gamma_{cc2}},\overline{\Gamma_{cc3}}\}$ optimistically designated ''cc'' for ''current conserving.'' Although gauge labels are not appended, full specification of these operators requires a choice of gauge also.

D. Distorted-wave impulse approximation

The DWIA for the electromagnetic transition amplitude that governs the single-nucleon knockout reaction $A(e,e'N)B$ can be expressed in the form [27]

$$\mathcal{M}=\int\frac{d^3q'}{(2\pi)^3}\,\mathcal{J}^e_\mu(\mathbf{q}')\,\frac{1}{Q'^2}\,\mathcal{J}^\mu_N(\mathbf{q}'), \tag{15}$$

where the electron and nuclear currents are

$$\mathcal{J}^e_\mu(\mathbf{q}')=\int d^3r\,e^{-i\mathbf{q}'\cdot\mathbf{r}}\overline{\psi^e_f}(\mathbf{r})\gamma_\mu\psi^e_i(\mathbf{r}), \tag{16a}$$

$$\mathcal{J}^N_\mu(\mathbf{q}')=\int d^3r\,e^{i\tilde{\mathbf{q}}'\cdot\mathbf{r}}\overline{\psi^N_f}(\mathbf{r})\Gamma_\mu\psi^N_i(\mathbf{r}), \tag{16b}$$

and where Γ_μ is the vertex operator for the nucleon current. In these expressions the electron wave functions relative to the target of mass m_A are denoted by the spinors ψ^e_i and ψ^e_f for the initial and final states, respectively. At this stage we leave implicit the dependence of the nuclear current upon the ejectile kinematics and the state of the residual nucleus. Since it is more convenient to express the ejectile wave functions ψ^N relative to the residual nucleus of mass m_B, the radial scale is adjusted by means of the reduced momentum transfer [32] $\tilde{\mathbf{q}}'=\mathbf{q}'m_B/m_A$.

If we assume that a virtual photon with momentum $\mathbf{q}'$ is absorbed by a single nucleon with initial momentum $\mathbf{p}$, the nuclear current at position $\mathbf{r}$ becomes

$$\mathcal{J}^N_\mu(\mathbf{r})=\int\frac{d^3p}{(2\pi)^3}\frac{d^3p''}{(2\pi)^3}\,e^{-i\tilde{\mathbf{q}}'\cdot\mathbf{r}}\tilde{\chi}^{(-)*}(\mathbf{p}',\mathbf{p}'')\times\Gamma_\mu(\mathbf{p}'',\mathbf{p})\tilde{\phi}(\mathbf{p}), \tag{17}$$

where the single-nucleon wave function is the amplitude for removing a nucleon from the initial state of target A and reaching the final state of residual nucleus B, such that

$$\tilde{\phi}(\mathbf{p})=\langle B|a(\mathbf{p})|A\rangle. \tag{18}$$

The distorted wave $\tilde{\chi}^{(-)*}(\mathbf{p}',\mathbf{p}'')$ is the amplitude that the ejectile with initial momentum $\mathbf{p}''=\mathbf{p}+\mathbf{q}'$ emerges from the nuclear field with final momentum $\mathbf{p}'$. Inclusion of inelastic processes within the final-state interactions can be accomplished using a coupled-channels model of the distorted waves, as discussed in Ref. [1]. In coordinate space these wave functions are expressed as

$$\phi(\mathbf{r})=\int\frac{d^3p}{(2\pi)^3}\,e^{i\mathbf{p}\cdot\mathbf{r}}\tilde{\phi}(\mathbf{p}), \tag{19a}$$

$$\chi(\mathbf{p}',\mathbf{r}) = \int \frac{d^3p''}{(2\pi)^3}\, e^{i\mathbf{p}''\cdot\mathbf{r}} \widetilde{\chi}(\mathbf{p}',\mathbf{p}''). \tag{19b}$$

Thus, the nuclear current becomes

$$\mathcal{J}^N_\mu(\mathbf{q}') = \int \frac{d^3p}{(2\pi)^3}\, \widetilde{\chi}^{(-)*}(\mathbf{p}',\mathbf{p}+\mathbf{q}')\Gamma_\mu(\mathbf{p}+\mathbf{q}',\mathbf{p})\widetilde{\phi}(\mathbf{p}), \tag{20}$$

where $\mathbf{q}'$ is the local momentum transfer supplied by the electron.

In the absence of Coulomb distortion, the electron current would be proportional to $\delta^3(\mathbf{q}'-\mathbf{q})$, so that the nuclear current could be evaluated for a unique value of the momentum transfer obtained from asymptotic kinematics. Fortunately, even in the presence of Coulomb distortion, the electron current tends to be sharply peaked about a local or effective momentum transfer, $\mathbf{q}' \approx \mathbf{q}_{\rm eff}$, so that for light nuclei it remains a good approximation [33] to evaluate the vertex function in the asymptotic momentum approximation (AMA),

$$\Gamma_\mu(\mathbf{p}'',\mathbf{p}) \approx \Gamma_\mu(\mathbf{p}',\mathbf{p}_m). \tag{21}$$

The effect of Coulomb distortion can be included in a somewhat better effective momentum approximation (EMA),

$$\Gamma_\mu(\mathbf{p}'',\mathbf{p}) \approx \Gamma_\mu(\mathbf{p}',\mathbf{p}_{m,\rm eff}), \tag{22}$$

where the effective missing momentum $\mathbf{p}_{m,\rm eff}=\mathbf{p}'-\mathbf{q}_{\rm eff}$ is based upon the the effective momentum transfer $\mathbf{q}_{\rm eff}=\mathbf{k}_i-\mathbf{k}_f$ obtained by replacing the asymptotic momenta k by local momenta k accelerated by the mean electrostatic potential, such that [34]

$$\overline{\mathbf{k}} = \mathbf{k} + f_Z \frac{\alpha Z}{R_Z}\hat{\mathbf{k}}, \tag{23}$$

where $f_Z = 1.5$ corresponds to the electrostatic potential at the center of a uniformly charged sphere of radius R_Z. Focusing of the electron wave function is then included by applying factors of k/k to each electron spinor [33]. We find that ambiguities in the one-body current operator are sufficiently large that the considerable computational effort required to improve upon AMA or EMA by treating the momenta in the vertex functions as operators is not justified [35]. Because we consider in this paper only light nuclei and high-energy electrons, we employ the AMA and omit electron distortion in the present calculations.

Therefore, we obtain

$$\mathcal{J}^N_\mu(\mathbf{q}') \approx \mathcal{J}^N_\mu(\mathbf{p}',\mathbf{q}_{\rm eff}) = \int d^3r\, e^{i\tilde{\mathbf{q}}_{\rm eff}\cdot\mathbf{r}} \chi^{(-)*}(\mathbf{p}',\mathbf{r}) \times \Gamma_\mu(\mathbf{p}',\mathbf{p}'-\mathbf{q}_{\rm eff})\phi(\mathbf{r}), \tag{24}$$

where the vertex function has now been reduced to a matrix, acting on nucleon spins, whose elements are evaluated using effective kinematics. This approach greatly simplifies the numerical evaluation of the transition amplitude and is a suitable starting point for nonrelativistic models that use nonrelativistic wave functions χ and ϕ and a nonrelativistic reduction of Γ. It also has the advantage of preserving the response function structure of the one-photon exchange approximation.

In the present work we evaluate the distorted waves using the Schrödinger equation with relativistic kinematics. Optical potentials are based upon phenomenological analysis of nucleon elastic scattering or upon empirical density-dependent effective interactions fitted to elastic and inelastic scattering data. Optical potentials from Dirac phenomenology can be transformed to Schrödinger-equivalent form and used with a Darwin nonlocality factor. Further details can be found in Ref. [1]. Unless stated otherwise, we use the $\overline{\Gamma}_{\rm cc1}$ vertex function with nucleon form factors from the model 3 of Gari and Krümpelmann [36,37].

E. Overlap functions

The single-nucleon overlap function $\phi(\mathbf{r})$ is expected to resemble strongly a single-particle eigenfunction in the mean field of the residual nucleus. In fact, one does find that Hartree-Fock wave functions provide excellent predictions for $(e,e'p)$ for strong states and modest missing momentum. Therefore, experimental data are usually analyzed using Woods-Saxon wave functions, modified by a Perey factor, where the radius is fitted to the shape of the momentum distribution and the potential depth is adjusted to reproduce the separation energy.

The quasiparticle Hamiltonian model of Ma and Wambach [7,8] provides a physically appealing model of both short-range and long-range correlations that is sufficiently simple for use in the analysis of experimental data. Here we provide a brief description of this model and refer to [1] for a more detailed review and comparison with related approaches. According to the model, the local effective mass $m^*(r)$ consists of two factors: (1) The k mass, $m_k(r)$ represents the spatial nonlocality of the mean field arising primarily from exchange effects, and (2) the E mass $m_E(r)$ represents temporal nonlocalities arising from short-range and tensor correlations and from coupling to surface modes. Thus, the effective mass is parametrized as

$$\frac{m^*(r)}{m} = \frac{m_k(r)}{m}\,\frac{m_E(r)}{m}, \tag{25a}$$

$$\frac{m_k(r)}{m} = 1-\alpha g(r), \tag{25b}$$

$$\frac{m_E(r)}{m} = 1+\beta_v g(r) + \beta_s \frac{dg(r)}{dr}, \tag{25c}$$

where $g(r)$ describes the radial shape of the mean field and is conveniently represented as a Woods-Saxon function

$$g(r) = \frac{1}{\exp[(r-R)/a]+1}, \tag{26}$$

where $R = R_V(A-1)^{1/3}$ is the radius and a is the diffuseness of the single-particle potential; typically one chooses $R_V \approx 1.25$ fm and $a \approx 0.65$ fm.

The correlated single-particle wave function is now represented by

$$\phi(\mathbf{r}) \propto \sqrt{\frac{m^*(r)}{m}}\,\varphi(\mathbf{r}), \tag{27}$$

where $\varphi(\mathbf{r})$ is the corresponding uncorrelated eigenfunction of the single-particle potential. The effects of spatial versus temporal nonlocality can be examined separately by replacing m^* by either m_k or m_E, respectively. One then finds that the effect of spatial nonlocality, as represented by $m_k(r)$, on the shapes of missing momentum distributions for valence orbitals is quite modest and, when analyzing data, can partly be compensated by adjustment of the radius parameter. Moreover, $m_k(r)/m$ is very similar to the Perey factor that is usually included when analyzing $(e,e'p)$ data anyway. By contrast, the pronounced surface peak in $m_E(r)$ produces substantial enhancements of the cross section for $p_m \gtrsim 300$ MeV/c. This suggested enhancement has been the subject of several recent experiments and proposals. Therefore, one of the purposes of the present work is to investigate the extent to which this effect can be disentangled from uncertainties in the reaction model for single-nucleon knockout by electron scattering that tend to increase with p_m also.

Ma and Wambach [8] applied this model to analyze various single-particle properties of ^{208}Pb. The geometrical parameters R_V and a were chosen to fit the charge density. The volume-nonlocality parameters $\alpha=0.42$ and $\beta_v=0.2$ were chosen to produce $m^*/m=0.7$ in the interior based upon the Perey-Buck analysis of the effective mass [38,39]. The surface-nonlocality parameter $\beta_s=-3.0$ fm was adjusted to reproduce the experimental particle-hole gap and spin-orbit splitting. The quasiparticle strength for deep hole states observed in ^{208}Pb$(e,e'p)$ by Quint [40] was fitted also. Subsequently, Ma and Feng [41] obtained $\alpha=0.4$, $\beta_v=0.1$, and $\beta_s=-3.0$ fm for ^{40}Ca. Hence, it appears that the A dependence of these parameters is small. Therefore, although we have not fitted the single-particle properties of ^{16}O, for the purpose of comparing the sensitivity of ^{16}O$(e,e'N)$ to long-range versus short-range correlations, we employ $\alpha=0.4$, $\beta_v=0.1$, and $\beta_s=-3.0$ fm for ^{16}O also. We use single-particle potentials adjusted to reproduce the p-shell ^{16}O$(e,e'p)$ data of Leuschner *et al.* [42].

However, it is likely that the model of Ma and Wambach overestimates the effect of long-range correlations upon the missing momentum distributions for valence knockout. The dispersive optical model of Mahaux and Sartor [11] produces an effective mass of similar shape, but the surface enhancement for ^{208}Pb is considerably less pronounced. Furthermore, Mahaux and Sartor represent the quasiparticle wave function using $m_k(r)$ in place of $m_E(r)$ in Eq. (27) and relate the quasiparticle strength to the matrix element of $m_E(r)$ for those wave functions. Thus, in this approach temporal nonlocality affects the quasiparticle strength but does not enhance the missing momentum distribution at large p_m. The analysis of ^{208}Pb$(e,e'p)$ by Bobeldijk *et al.* [12] found that inclusion of $m_E(r)$ in the overlap function improves the agreement between DWIA calculations and the data for large p_m and found a slight preference for the milder surface peak of Mahaux and Sartor over the stronger surface peak of Ma and Wambach. However, subsequent work found comparable effects at large p_m arising from two-body currents [13] or from Gordon ambiguities in relativistic DWIA [14]. Furthermore, channel coupling in final-state interactions can also enhance knockout cross sections at large p_m [1]. Nevertheless, even though this model probably overestimates the influence of correlations on valence knockout, it provides an instructive guide to the importance of correlations at large p_m relative to ambiguities in the one-body current operator.

F. Observables and response functions for $A(\vec{e},e'\vec{N})B$

Nucleon knockout reactions of the type $A(\vec{e},e'\vec{N})B$ initiated by a longitudinally polarized electron beam and for which the ejectile polarization is detected may be described by a doubly differential cross section of the general form [43,44]

$$\frac{d\sigma_{hs}}{d\varepsilon_f d\Omega_e d\Omega_N} = \sigma_0 \frac{1}{2}[1+\boldsymbol{P}\cdot\boldsymbol{\sigma}+h(A+\boldsymbol{P}'\cdot\boldsymbol{\sigma})], \tag{28}$$

where ε_i (ε_f) is the initial (final) electron energy, σ_0 is the unpolarized cross section, h is the electron helicity, s indicates the nucleon spin projection upon $\boldsymbol{\sigma}$, $\boldsymbol{P}$ is the induced polarization, A is the electron analyzing power, and $\boldsymbol{P}'$ is the polarization transfer coefficient. Thus, the net polarization of the recoil nucleon $\boldsymbol{\Pi}$ has two contributions of the form

$$\boldsymbol{\Pi}=\boldsymbol{P}+h\boldsymbol{P}', \tag{29}$$

where $|h|\leqslant 1$ is interpreted as the longitudinal beam polarization. Each of the observables may be expressed in terms of kinematical factors $V_{\alpha\beta}$ and response functions $R_{\alpha\beta}$, as reviewed in Ref. [1].

The recoil polarization is usually calculated with respect to a helicity basis in the barycentric frame defined by the basis vectors

$$\hat{\boldsymbol{L}}=\frac{\boldsymbol{p}_N}{|\boldsymbol{p}_N|}, \tag{30a}$$

$$\hat{\boldsymbol{N}}=\frac{\boldsymbol{q}\otimes\hat{\boldsymbol{L}}}{|\boldsymbol{q}\otimes\hat{\boldsymbol{L}}|}, \tag{30b}$$

$$\hat{\boldsymbol{S}}=\hat{\boldsymbol{N}}\otimes\hat{\boldsymbol{L}}. \tag{30c}$$

However, since this basis is not well defined when $\boldsymbol{q}$ and $\boldsymbol{p}_N$ are either parallel or antiparallel, these cases are conventionally handled by first rotating the reaction plane to ϕ_N, as it would be in nonparallel kinematics, and then taking the limit $\theta_{pq}\rightarrow 0^\circ$ or $\theta_{pq}\rightarrow 180^\circ$ as required. Note that since the basis vectors $\hat{\boldsymbol{S}}$ and $\hat{\boldsymbol{N}}$ reverse directions when $\phi\rightarrow\phi+\pi$, the corresponding components of the recoil polarizations also tend to reverse sign even when there is no physical asymmetry with respect to ϕ; this behavior is simply an artifact of the basis.

Alternatively, since the recoil polarization is measured in the laboratory frame, it is useful to employ a polarimeter basis in which

$$\hat{\boldsymbol{y}}=\frac{\boldsymbol{k}_i\otimes\boldsymbol{k}_f}{|\boldsymbol{k}_i\otimes\boldsymbol{k}_f|}, \tag{31a}$$

TABLE I. Kinematics for the $^{16}O(e,e'p)^{15}N$ experiment of Blomqvist *et al.* [17].

Setting	q (MeV/c)	ω (MeV)	p_m (MeV/c)	Q^2 [(GeV/c)^2]	x	y (GeV/c)
2	550	202–259	83–183	0.255	0.70–0.49	0.074–0.123
3	470		163–253	0.165	0.47–0.33	0.157–0.247
4	390		251–331	0.095	0.27–0.18	0.245–0.325
5	315		326–386	0.045	0.13–0.09	0.322–0.383
6	495	214–255	376–496	0.192	0.49–0.38	0.156–0.217
7	315	217–273	526–676	0.039	0.10–0.07	0.350–0.405

$$\hat{\boldsymbol{x}}=\frac{\hat{\boldsymbol{y}}\otimes\boldsymbol{p}_N}{|\hat{\boldsymbol{y}}\otimes\boldsymbol{p}_N|} \tag{31b}$$

$$\hat{\boldsymbol{z}}=\hat{\boldsymbol{x}}\otimes\hat{\boldsymbol{y}} \tag{31c}$$

Furthermore, although the effect is small except for very light targets, the polarization vector must be transformed to the lab frame using a Wigner rotation [45]. One advantage of presenting the recoil polarization in the laboratory or polarimeter basis is that the recoil polarization components are continuous as $\mathbf{p}_N$ moves through $\mathbf{q}$ from one side to the other. Unlike $\hat{\boldsymbol{S}}$ and $\hat{\boldsymbol{N}}$, $\hat{\boldsymbol{x}}$ and $\hat{\boldsymbol{y}}$ do not reverse directions when $\phi\rightarrow\phi+\pi$. For coplanar quasiperpendicular kinematics with $\hat{\boldsymbol{y}}$ upwards, it has become conventional to assign positive missing momentum to ejectile momenta on the large-angle side of $\mathbf{q}$, such that $\phi=\pi$ and $\theta_{pq}>0$.

The distorted missing momentum distribution $\rho^D(\mathbf{p}_m,\mathbf{p}')$ is obtained by dividing the unpolarized differential cross section σ_0 by the elementary electron-nucleon cross section σ_{eN} for initial (final) nucleon momenta $\mathbf{p}_m$ ($\mathbf{p}'$), such that

$$\rho^D(\mathbf{p}_m,\mathbf{p}')=\frac{\sigma_0}{K\sigma_{eN}}, \tag{32}$$

where

$$\sigma_{eN}=\frac{\varepsilon_f}{\varepsilon_i}\frac{\alpha^2}{Q^4}\eta_{\mu\nu}\mathcal{W}^{\mu\nu}_{eN} \tag{33}$$

is based upon the PWIA response tensor for off-shell kinematics and, by convention, does not include the phase-space factor K. Ambiguities in the distorted momentum distribution are minimized by requiring consistency between the vertex function and gauge used to evaluate both the numerator and denominator of Eq. (32). However, because nature does not afford one the luxury of choosing these prescriptions for the experimental cross sections, it has become customary to report experimental data in the form of a reduced cross section defined by

$$\sigma_{\rm red}(\mathbf{p}_m,\mathbf{p}')=\frac{\sigma_0}{K\sigma_{cc1}}, \tag{34}$$

where σ_{cc1} is σ_{eN} obtained from $\overline{\Gamma}_{\rm cc1}$ using the Coulomb gauge. Therefore, when making comparisons with experimental data for the distorted momentum distribution, we use $\sigma_{\rm red}$ with the same denominator, usually $\sigma_{\rm cc1}$, that was used to analyze the data even if that denominator is inconsistent with the gauge or current operator used in the theoretical calculation of the numerator, namely, the cross section itself. Although direct comparisons between theoretical and experimental differential cross sections would be simpler to interpret, the reduced cross section depends less strongly on the kinematics of the experiment and strongly resembles the momentum distribution. Furthermore, the data are often reported only as reduced cross sections and the same purpose is served by defining $\sigma_{\rm red}$ with a common denominator for both theory and experiment.

III. RESULTS

A. $^{16}O(e,e'p)$ for Mainz kinematics

Blomqvist *et al.* [17] reported missing momentum distributions for the lowest $(1p_{1/2})^{-1}$ and $(1p_{3/2})^{-1}$ states for the $^{16}O(e,e'p)^{15}N$ reaction with ejectile kinetic energies in the range $190\lesssim T_p\lesssim 260$ MeV. These data were acquired using six kinematical settings summarized by Table I, where the Bjorken x is defined by $x=Q^2/2m\omega$ and the y-scaling variable by the solution of

$$\omega+m_A=\sqrt{m_N^2+(y+q)^2}+\sqrt{m_B^2+y^2}. \tag{35}$$

Although we recognize that the direct reaction mechanism based upon a one-body current operator may not suffice for small x or, equivalently, large positive y where meson-exchange and isobar currents become important, several previous analyses attempted to interpret the data for large p_m in terms of single-nucleon momentum components. Here we consider gauge and Gordon ambiguities in the direct knockout contribution.

1. Normalization issue

Calculations illustrating the sensitivity of DWIA calculations to the choice of optical model are shown in Fig. 1. The calculations were made using the Coulomb gauge and the overlap wave functions and spectroscopic factors fitted to the data of Leuschner *et al.* [42] acquired at NIKHEF using $T_p\approx 100$ MeV. For simplicity, these calculations were performed for parallel kinematics using a constant ejectile energy of $T_p=215$ MeV; more detailed calculations using the proper experimental kinematics are practically indistinguishable over this range of missing momentum. We compare the EDAD1 potential fitted by Cooper *et al.* [46] using Dirac phenomenology, the potential of Schwandt *et al.* [47] fitted to proton elastic scattering for $A\geqslant 40$ and $80\leqslant T_p\leqslant 180$ MeV, and a folding model potential based upon an empirical effective interaction (EEI) fitted to proton-nucleus

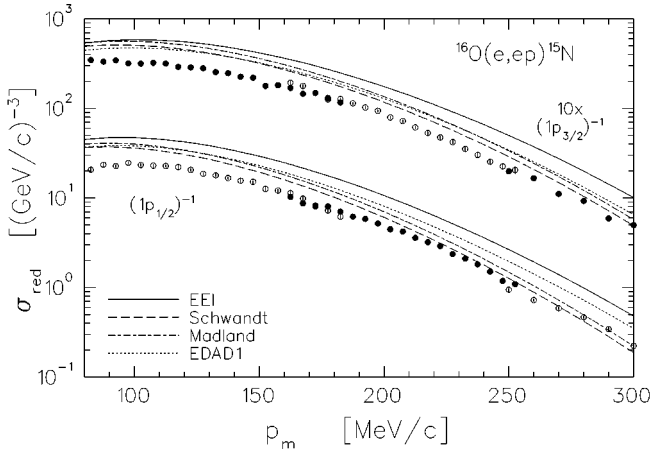

FIG. 1. Normalization problem for Mainz ^{16}O$(e,e'p)$ at $T_p \sim 215$ MeV. The data of Blomqvist *et al.* [17] are shown with alternating groups of solid versus open symbols corresponding to successive kinematic settings. DWIA calculations for parallel kinematics with $T_p = 215$ MeV use the overlap functions fitted to data of Leuschner *et al.* [42] for $T_p \approx 100$ MeV. The optical potentials are EEI [48] for solid, Schwandt [47] for long dashed, Madland [50] for dot-dashed, or EDAD1 [46] for dotted lines.

elastic and inelastic scattering data for 200 MeV [48]. The properties of these potentials are compared in detail in Refs. [1,49], wherein we find that the EEI model gives the best predictions for nuclear transparency while the EDAD1 potential is too absorptive. However, although many $(e,e'p)$ calculations use the Schwandt potential significantly outside the ranges of mass and/or energy for which it was optimized, we find that its properties become unreasonable when extrapolated in energy. Therefore, we also include a variation of the Schwandt model by Madland [50] that extends the upper limit of its energy range from 180 MeV to 400 MeV and the lower limit of its mass range from 40 down to 12.

We find that all calculations overestimate the peak of the missing momentum distribution and must be scaled by factors of about 0.5–0.6 to reproduce the data for low p_m. The EEI and EDAD1 potentials give distributions of similar shape which both describe the data well if the calculations are reduced by factors of about 0.5 or 0.6, respectively. The EEI requires a smaller scale factor than the more absorptive EDAD1 potential, but is nevertheless expected to be more reliable because it provides more accurate predictions for nuclear transparency and for proton absorption and neutron total cross sections [49]. The Schwandt and Madland potentials require intermediate normalization factors for small p_m, but predict cross sections which fall more rapidly than the data as p_m increases. The failure of those potentials to reproduce the shape of the missing momentum distribution can be attributed to their simplistic radial shapes, whereas the more complicated radial shapes produced by folding a nuclear density with a density-dependent effective interaction or by reducing a Dirac optical potential to Schrödinger-equivalent form tend to enhance the cross section at large p_m. Although we might prefer to employ the EEI potential, that interaction is only available at discrete energies. The calculations for larger p_m are more sensitive to the details of the kinematical conditions and hence require optical potentials over a broad range of energy. Therefore, we chose to use the EDAD1 potential for the calculations that follow despite the fact that its absorption is somewhat too strong. These calculations are scaled by a factor of 0.6 based upon small p_m.

These data were reported in the form of reduced cross sections where σ_{ep} was calculated using $\overline{\Gamma}_{cc1}$ according to the Coulomb gauge. Hence, the calculations for reduced cross sections shown in Fig. 1 use the same denominator that was reportedly used to analyze the data. Regrettably, the actual differential cross section data do not appear to be available. Hence, the normalization problem might be related to a possible discrepancy in the calculation of σ_{ep} or the phase-space factor. Although we consider this possibility to be unlikely, we would like to take this opportunity to encourage experimentalists to make the original differential cross sections available directly before constructing ratios that are not necessarily unambiguous.

The discrepancy between these calculations and the small-p_m data for 200 MeV is a serious problem. Blomqvist *et al.* also performed measurements for $T_p \approx 100$ MeV using the same waterfall target and obtained good agreement with the data of Leuschner *et al.* Thus, there is a discrepancy of about a factor of 2 between the spectroscopic factors one would deduce from the 100 and 215 MeV data using the same reaction model for each. The spectroscopic factors obtained by Leuschner *et al.* are consistent with the systematics for valence hole states established over a broad mass range [1], whereas those suggested by the experiment of Blomqvist *et al.* would be anomalously small for ^{16}O. Note that the calculations reported in Refs. [17,6] using the Schwandt potential, despite its inapplicability, show essentially the same normalization problem. Therefore, if these data are normalized correctly, there may be a serious error in the DWIA even when the kinematics are nearly quasifree. It is important to confirm these data and to extend the range of ejectile energy upwards. In the meantime, we present DWIA calculations for the full kinematical range of the Mainz experiment normalized to the data for small p_m.

2. Gauge ambiguities

The sensitivity of missing momentum distributions for the Mainz ^{16}O$(e,e'p)^{15}$N experiment to the choice of gauge is illustrated in Fig. 2. These calculations were performed for the actual kinematics of the experiment and hence there are discontinuities between settings. All calculations employ the $\overline{\Gamma}_{cc1}$ current operator and the EDAD1 potential and are scaled by a factor of 0.6. The data for successive settings are shown alternating between filled and open symbols. In order to compare our calculations directly with the experimental data, reduced cross sections, σ_{red}, were based upon the same denominator that was used to analyze the data, namely $\overline{\Gamma}_{cc1}$ in Coulomb gauge, even when the numerator uses the Landau or Weyl gauges.

Our calculations using the Coulomb gauge are somewhat larger for $p_m \gtrsim 300$ MeV/c than the comparable results of Refs. [17,6], normalized in the same manner at low-p_m, because we employ the EDAD1 potential instead of the Schwandt potential. Nevertheless, calculations using the Coulomb gauge, in which the longitudinal current is modified to restore current conservation, tend to remain below the data. Furthermore, calculations using the Weyl gauge, in

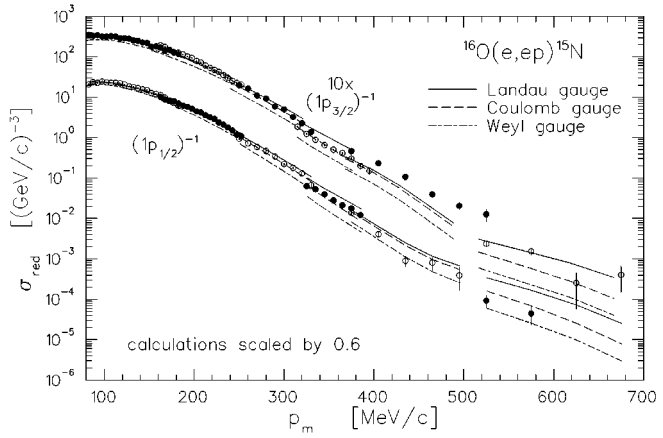

FIG. 2. Sensitivity of Mainz data for $^{16}\mathrm{O}(e,e'p)$ at $T_p \sim 215$ MeV to choice of gauge. The data of Blomqvist *et al.* [17] are shown with alternating groups of solid versus open symbols corresponding to successive kinematic settings. DWIA calculations for the experimental kinematics were made using the EDAD1 potential [46] and overlap functions from Leuschner *et al.* [42]. All calculations were scaled by a factor of 0.6. Solid, dashed, and dot-dashed lines use the Landau, Coulomb, or Weyl gauges, respectively. Discontinuities correspond to substantial changes in kinematical conditions.

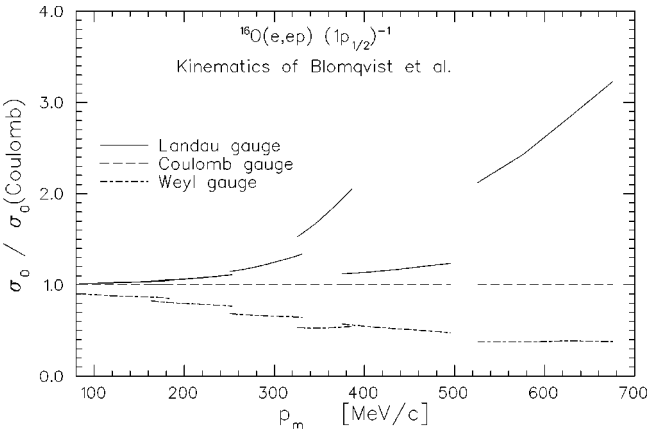

FIG. 3. The sensitivity of DWIA calculations for the $^{16}\mathrm{O}(e,e'p)$ reaction at the kinematics of the Mainz experiment for $T_p \sim 215$ MeV to the choice of gauge are illustrated by ratios with respect to results for the Coulomb gauge. Solid, dashed, and dot-dashed lines use the Landau, Coulomb, or Weyl gauges, respectively. Discontinuities correspond to substantial changes in kinematical conditions.

which the scalar current is modified instead, give somewhat smaller cross sections for modest p_m and fall even lower for large missing momentum. Of course, those calculations would have agreed if the model conserved current and there exists no rigorous criteria for choosing one over another. On the other hand, calculations using the Landau gauge tend to give larger cross sections than the traditional Coulomb gauge and give better agreement with these data. Unfortunately, better agreement with data does not necessarily constitute a preference because these kinematics for large p_m are too far from quasifree to ensure dominance of the one-body current or the direct knockout mechanism.

The differences between these models can be illustrated more clearly by Fig. 3 which shows the ratio with respect to the standard calculation using the Coulomb gauge. At small p_m the Landau and Coulomb gauges give very similar results, with the Weyl gauge falling about 10% lower. The ratio σ(Weyl)/σ(Coulomb) tends to decrease steadily as p_m increases with minor discontinuities between kinematical settings, whereas σ(Landau)/σ(Coulomb) increases with marked discontinuities where the scaling variables change abruptly. Notice that σ(Landau)/σ(Coulomb) is closer to unity when $p_m \sim 400$ MeV/c than when $p_m \sim 300$ MeV/c because $x \sim 0.45$ for the former versus $x \sim 0.11$ for the latter. Nevertheless, the net effect is a widening spread between these models as p_m increases; for large p_m and small x, the discrepancy between the Landau and Weyl gauges approaches an order of magnitude.

In Fig. 4 we compare cross sections for the $\overline{\Gamma}_{cc2}$ and $\overline{\Gamma}_{cc3}$ vertex functions with those for $\overline{\Gamma}_{cc1}$, all using the Coulomb gauge. We find that Gordon ambiguities remain relatively small, within $\pm 10\%$, even though x becomes quite small for some kinematics. The abrupt change for $p_m \gtrsim 375$ MeV/c occurs at the transition between nearly parallel and markedly nonparallel kinematical conditions. Within each kinematic range the Gordon ambiguities increase with p_m as the kinematics move further off shell. Nevertheless, Gordon ambiguities for the nonrelativistic DWIA appear to be much less important than gauge ambiguities for small Q^2. On the other hand, Gordon ambiguities can be much larger for DWIA calculations which evaluate ejectile distortion in a Dirac framework. For example, Udías *et al.* [14] compared calculations for the ^{208}Pb$(e,e'p)$ data of Bobeldijk *et al.* [12] based upon a relativistic DWIA model using the $\overline{\Gamma}_{cc1}$ and $\overline{\Gamma}_{cc2}$ operators and find differences that increase from 10% at small p_m and reach almost an order of magnitude for $p_m \sim 500$ MeV/c, whereas nonrelativistic DWIA calculations for the same conditions find variations that remain within a few percent. The greater sensitivity of relativistic DWIA calculations to Gordon ambiguities arises from the distortion of the spinors by the strong Dirac scalar and vector potentials,

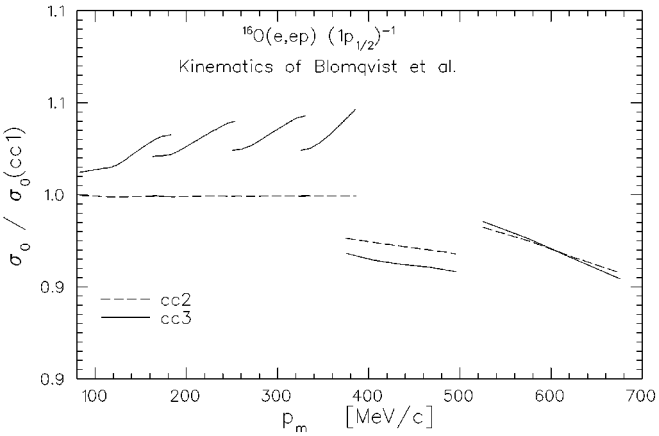

FIG. 4. The sensitivity of DWIA calculations of differential cross sections for the $^{16}\mathrm{O}(e,e'N)(1p_{1/2})^{-1}$ reaction at the kinematics of the Mainz experiment to the choice of vertex function is illustrated by ratios with respect to results for the cc1 operator in the Coulomb gauge. Dashed and solid lines use the cc2 or cc3 operators, respectively.

which upsets some delicate relationships between upper and lower components that enter matrix elements of the current operator [51].

In addition, there are ambiguities due to optical potentials and effects of channel coupling in final-state interactions [1] that also become important at large p_m. Furthermore, two-body currents due to meson-exchange and intermediate-isobar excitation can substantially increase the cross section at large p_m relative to the one-body current [52,13]. In particular, van der Sluys *et al.* [13] found using the HF-RPA approach that two-body currents produce effects upon $^{208}\mathrm{Pb}(e,e'p)$ at large p_m as large or larger than the effects attributed to long-range correlations by Bobeldijk *et al.* [12]. Therefore, under these conditions, DWIA calculations of the cross section become completely unreliable and no conclusion can be drawn about correlations in the nuclear wave function.

B. Quasifree $^{16}\mathrm{O}(\vec{e},e'\vec{N})$ for $q=1.0$ GeV/c

An experiment that is about to run at TJNAF [15] seeks to measure high-momentum components in $^{16}\mathrm{O}(e,e'p)^{15}\mathrm{N}$ using quasifree kinematics for $\omega=0.445$ GeV, $q=1.0$ GeV/c such that $Q^2=0.8$ (GeV/c)^2 and $x=0.96$. The larger beam energy $E_0=2.445$ GeV makes it possible to reach large p_m with $x\approx 1$. A related experiment [16] will measure recoil polarization at modest p_m using the $^{16}\mathrm{O}(\vec{e},e'\vec{p})^{15}\mathrm{N}$ reaction with similar kinematics. Hence, it is of interest to examine the relative importance of gauge ambiguities under those conditions. For completeness, we also consider the $^{16}\mathrm{O}(\vec{e},e'\vec{n})^{15}\mathrm{O}$ reaction. The calculations are performed in quasiperpendicular kinematics, constant $(\omega,\mathbf{q})$, and are displayed as functions of missing momentum where positive p_m refers to ejectile angles on the large-angle side of $\mathbf{q}$, $\theta_p > \theta_q$, and negative p_m to $\theta_p < \theta_q$. The EDAD1 potential from Dirac phenomenology [46] was used.

1. Differential cross section

Figure 5 shows the ratio with respect to Coulomb gauge for ground-state cross sections in quasiperpendicular kinematics. As $|p_m|$ approaches 500 MeV/c, the Weyl/Coulomb ratio for proton knockout approaches 0.5 for positive or 2.0 for negative p_m, whereas the corresponding ratio for the Landau gauge remains within about $\pm 15\%$ of unity when $x\approx 1.0$. The gauge dependence for neutron knockout is similar but somewhat stronger. Similarly, in Fig. 6 we examine the dependence of single-nucleon knockout cross sections upon the prescription for off-shell extrapolation of the one-body current operator using the customary Coulomb gauge. For valence states, ambiguities due to violation of the Gordon identity remain below about 10% for $p_m \lesssim 250$ MeV/c but reach about 35% as p_m approaches 500 MeV/c. The Gordon ambiguities are substantially stronger for $Q^2=0.8$ (GeV/c)^2 than for the low-Q^2 Mainz experiment because such violations are relativistic effects. Therefore, differential cross sections suffer from serious gauge and off-shell ambiguities at large missing momentum with gauge ambiguities being exacerbated for small x and Gordon ambiguities increasing with Q^2.

It is important to recognize that these ambiguities are properties of the current operator that are not significantly affected by optical-model distortion, at least in the context of nonrelativistic models. Calculations using plane waves for the ejectile are smoother but otherwise very similar to those shown here—optical-model distortion merely produces gentle oscillations about the plane-wave curves. Therefore, it might be possible to improve the model of the current operator without requiring a very detailed description of the final-state interactions.

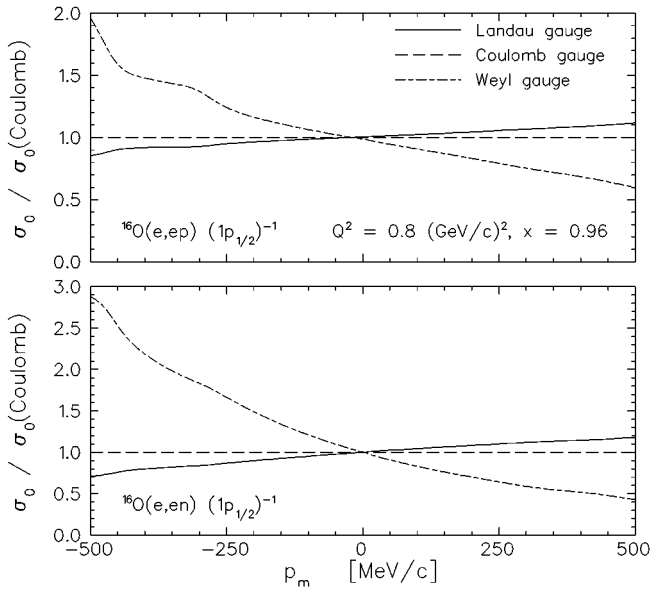

FIG. 5. The sensitivity of DWIA calculations of differential cross sections for the $^{16}\mathrm{O}(e,e'N)(1p_{1/2})^{-1}$ reaction at the kinematics of the TJNAF proposal No. 89-003 to the choice of gauge is illustrated by ratios with respect to results for the Coulomb gauge. Solid, dashed, and dot-dashed lines use the Landau, Coulomb, or Weyl gauges, respectively.

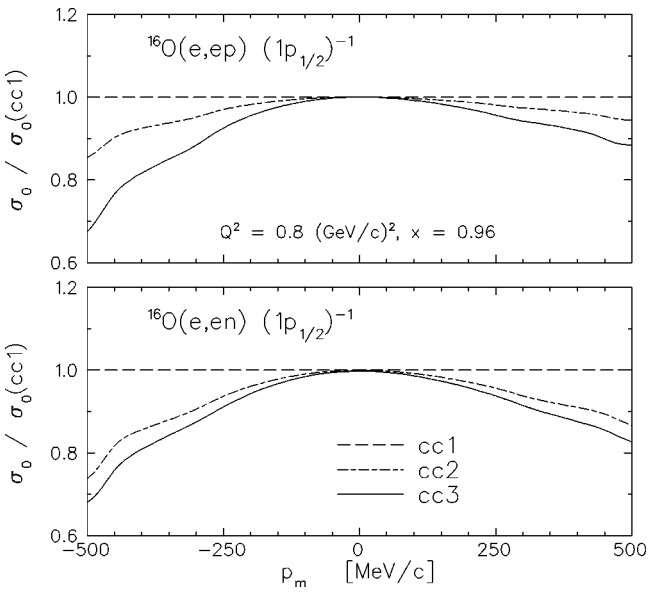

FIG. 6. The sensitivity of DWIA calculations of differential cross sections for the $^{16}\mathrm{O}(e,e'N)(1p_{1/2})^{-1}$ reaction at the kinematics of the TJNAF proposal No. 89-003 to the choice of vertex function is illustrated by ratios with respect to results for the cc1 operator in the Coulomb gauge. Dashed, dot-dashed, and solid lines use the cc1, cc2, or cc3 operators, respectively.

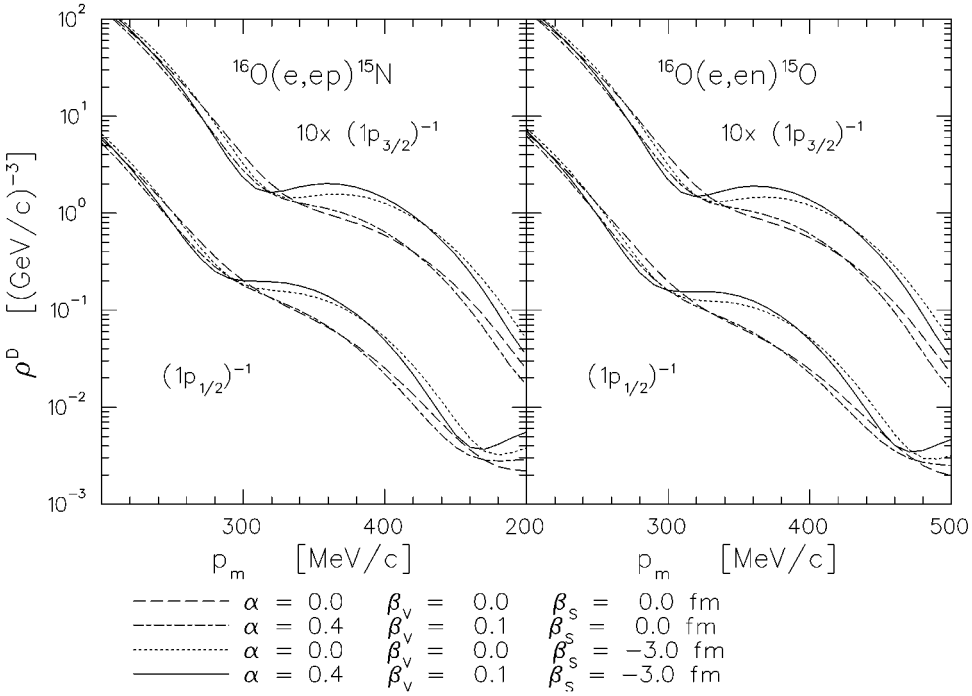

FIG. 7. The sensitivity of DWIA calculations to correlations is illustrated by differential cross sections for the $^{16}\mathrm{O}(e,e'N)(1p)^{-1}$ reaction at large p_m for the kinematics of the TJNAF proposal No. 89-003. Dashed lines use the basic Woods-Saxon wave function, dash-dotted lines include $m_k(r)$, dotted lines include $m_E(r)$, and solid lines include $m^*(r)$.

The magnitude of these ambiguities poses serious problems for experiments which seek to interpret cross section measurements for valence single-nucleon knockout in terms of correlations. This problem is illustrated by Fig. 7, which shows the effect of m_k and m_E corrections to the overlap functions at large missing momentum. In Fig. 8 we illustrate the effect of m_k and m_E corrections using ratios between the missing momentum distributions with respect to the Woods-Saxon model. Although this model is rather simple, it should suffice to indicate the relative sensitivity of missing momentum distributions to long-range versus short-range correlations. It is clear that the short-range correlations represented by $m_k(r)$ have relatively little effect upon the shape of the missing momentum distribution and that this minor modulation would be reduced when analyzing experimental data simply by readjusting the radius parameter for the Woods-Saxon potential. On the other hand, long-range correlations represented by $m_E(r)$ produce a relatively strong enhancement that is sufficiently localized in missing momentum to survive the customary fitting procedure. If the long-range correlations do affect momentum distributions for valence states this strongly and the reaction model were under good control, it should be possible to extract the parameters describing $m_E(r)$ from cross section data. However, the effects of these correlations are not substantially larger than the ambiguities in cross section due to the current operator. Moreover, we have argued that it is likely that the Ma and Wambach model overestimates correlations for valence states. Hence, it will be necessary to achieve a much more accurate understanding of the one-body current operator in the nuclear environment before one can expect to extract structure information from relatively small modulations of the differential cross section for single-nucleon knockout.

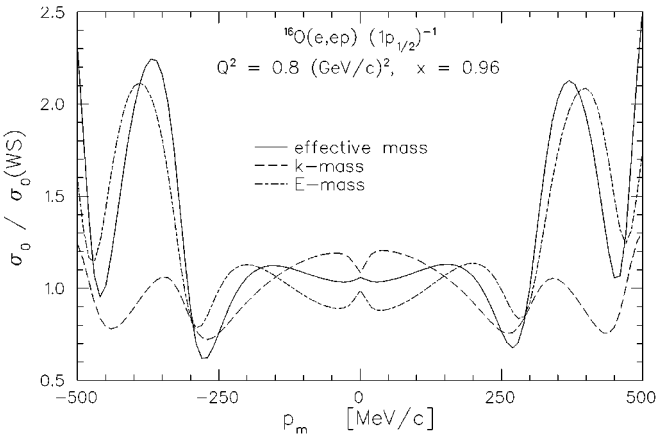

FIG. 8. The sensitivity of DWIA calculations of differential cross sections for the $^{16}\mathrm{O}(e,e'p)(1p)^{-1}_{1/2}$ reaction to correlations is illustrated for the kinematics of the TJNAF proposal No. 89-003 by ratios with respect to the missing momentum distribution for the basic Woods-Saxon wave function. Dashed lines include $m_k(r)$, dash-dotted lines include $m_E(r)$, and solid lines include $m^*(r)$.

Furthermore, relativistic DWIA models are considerably more sensitive to Gordon ambiguities than are nonrelativistic models. In addition, channel coupling in final-state interactions can produce significant state-dependent changes of cross section in the same range of missing momentum. It does not appear likely that one will be able to extract correlation information from single-nucleon knockout for valence states. On the other hand, a wide variety of theoretical calculations suggest that short-range and tensor correlations should yield considerable high-momentum strength at large missing energies, well beyond the ranges relevant to the

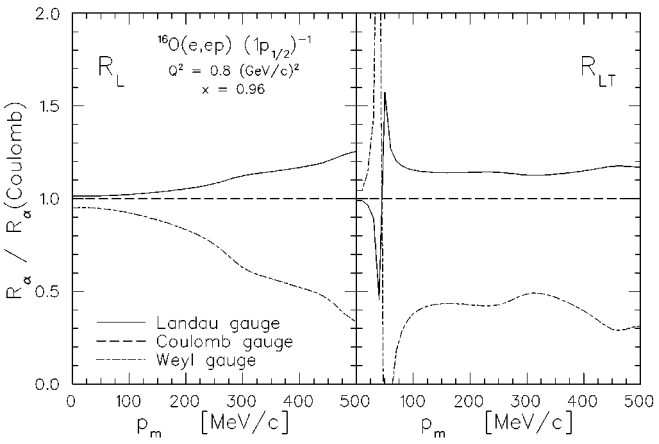

FIG. 9. The sensitivity of DWIA calculations of the R_L and R_{LT} response functions for the $^{16}\mathrm{O}(e,e'p)(1p_{1/2})^{-1}$ reaction at the kinematics of the TJNAF proposal No. 89-003 to the choice of gauge is illustrated by ratios with respect to results for the Coulomb gauge. Solid, dashed, and dot-dashed lines use the Landau, Coulomb, or Weyl gauges, respectively.

mean field. For example, Polls *et al.* [6] evaluated the hole spectral function for $^{16}\mathrm{O}(e,e'p)$ and found that large momenta occur predominantly at large missing energy, such that the continuum strength is more than an order of magnitude greater than the quasihole strength for $p_m \gtrsim 400$ MeV/c. However, further investigation is needed to determine whether the spectral function actually can be extracted from $(e,e'p)$ data for large p_m and E_m despite ambiguities in the current operator and final-state interactions under these conditions.

2. Response functions

Since gauge differences between these currents are confined to the scalar and longitudinal currents, it is also useful to examine the dependence of the R_L and R_{LT} response functions upon the choice of gauge. These response functions for $^{16}\mathrm{O}(e,e'p)(1p_{1/2})^{-1}$ are shown in Fig. 9 as ratios with respect to the Coulomb gauge using the Γ_{cc1} operator. For R_L we find that the gauge dependence increases steadily with p_m, but for R_{LT} we find nearly constant ratios except in the immediate vicinity of a node. Similarly, Picklesimer *et al.* [19] report significant gauge ambiguities in R_L for $Q^2 \approx 0.25$ (GeV/c)^2 using a relativistic DWIA calculation.

A useful way to minimize nuclear structure ambiguities when studying the current operator is provided by the left-right asymmetry

$$A_\phi = \frac{\sigma(\phi=0)-\sigma(\phi=\pi)}{\sigma(\phi=0)+\sigma(\phi=\pi)}, \tag{36}$$

in which uncertainties in the overlap function or optical potential tend to divide out of the ratio. The gauge dependence of A_ϕ for $^{16}\mathrm{O}(e,e'p)(1p_{1/2})^{-1}$ is shown in Fig. 10. We again find that the Landau and Coulomb gauges give rather similar results for quasifree kinematics, whereas the Weyl gauge differs significantly. On the other hand, Fig. 11 compares A_ϕ for the $\{\Gamma_{\mathrm{cc1}},\Gamma_{\mathrm{cc2}},\Gamma_{\mathrm{cc3}}\}$ vertex functions within the Coulomb gauge and shows that the left-right asymmetry is relatively insensitive to the violations of the Gordon identity

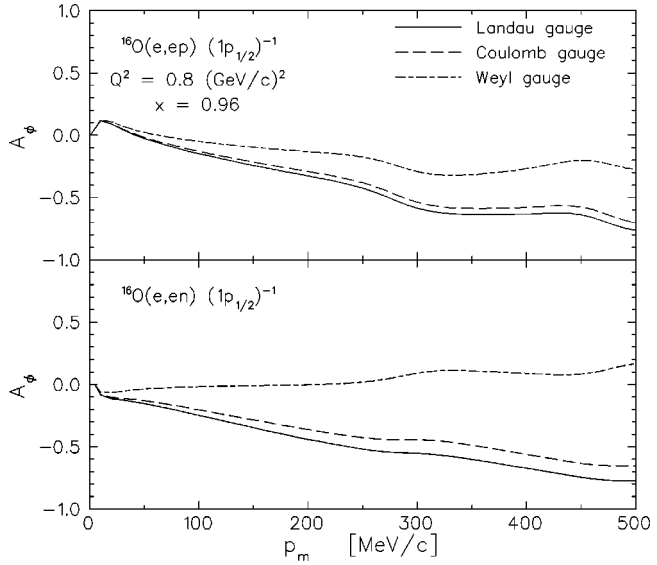

FIG. 10. The sensitivity of DWIA calculations of the left-right asymmetry for the $^{16}\mathrm{O}(e,e'N)(1p_{1/2})^{-1}$ reaction at the kinematics of the TJNAF proposal No. 89-003 to the choice of gauge is illustrated by ratios with respect to results for the Coulomb gauge. Solid, dashed, and dot-dashed lines use the Landau, Coulomb, or Weyl gauges, respectively.

by off-shell current operators. Evidently, these prescriptions for current conservation and off-shell extrapolation affect the dependences of the differential cross section more strongly for the polar angle than for the azimuthal angle. However, there is probably a greater spread among A_ϕ calculations in relativistic DWIA because Gordon ambiguities are larger (cf. Fig. 3 of Ref. [14]). Furthermore, by changing the direction of the effective momentum transfer $\mathbf{q}_{\mathrm{eff}}$, electron distortion can mix polar and azimuthal angles and produce significant changes in R_{LT} and A_ϕ, particularly for heavy targets [53]. However, investigation of the coupling between electron distortion and ambiguities in the nucleon current is beyond the scope of the present work.

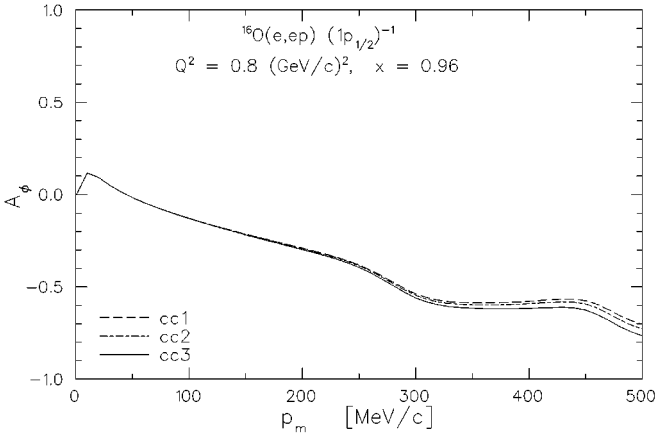

FIG. 11. The sensitivity of DWIA calculations of the left-right asymmetry for the $^{16}\mathrm{O}(e,e'N)(1p_{1/2})^{-1}$ reaction at the kinematics of the TJNAF proposal No. 89-003 to the choice of vertex function is illustrated by ratios with respect to results for the cc1 operator in the Coulomb gauge. Dashed, dot-dashed, and solid lines use the cc1, cc2, or cc3 operators, respectively.

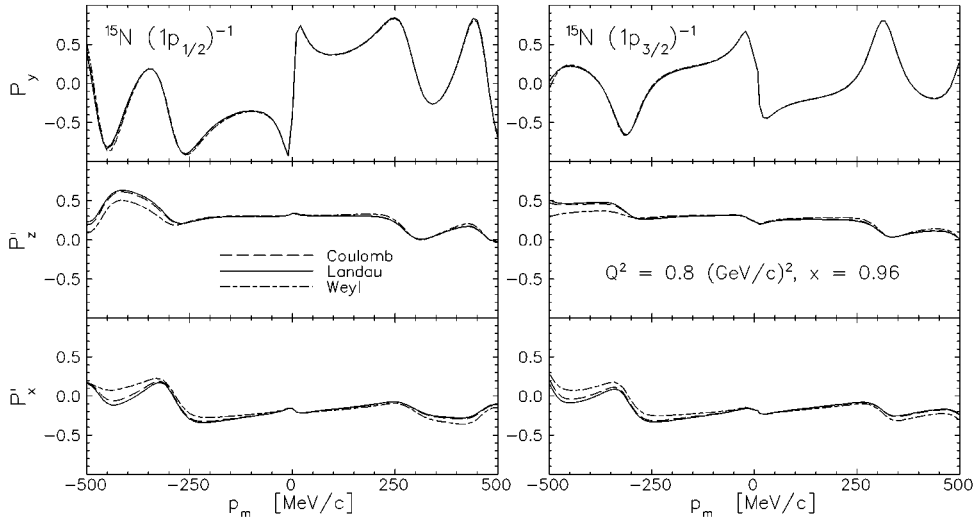

FIG. 12. DWIA calculations of recoil polarization for the ^{16}O$(\vec{e},e'\vec{p})$ reaction at the kinematics of TJNAF proposal No. 89-033 are shown using the cc1 current operator. Solid, dashed, and dot-dashed lines use the Landau, Coulomb, or Weyl gauges, respectively.

Although the dependence of A_ϕ upon gauge is indicative of a failure of the DWIA, it may nevertheless be possible to select the most appropriate gauge by this criterion. This measure of the azimuthal asymmetry is sensitive to properties of the current operator that are relatively insensitive to the structure of the target. Therefore, one can hope that one particular choice of gauge might provide the best predictions for this quantity over a wide range of targets and kinematical conditions, provided that the one-body current is dominant. Unfortunately, there exists very little data for R_{LT} in single-nucleon knockout from complex nuclei; see Ref. [1] for a review of the data for ^{16}O$(e,e'p)$ at $Q^2=0.2$ [54] and $Q^2=0.3$ (GeV/c)^2 [55]. Both data sets suggest that the azimuthal asymmetry is somewhat larger than obtained in DWIA using the Coulomb gauge, but theoretical calculations suggest that meson-exchange and isobar contributions are important. However, the Pavia [56,57] and Gent [58] groups make very different predictions for the relative importance of meson-exchange versus isobar currents and for the dependence of two-body currents upon nuclear structure.

Although gauge ambiguities at large p_m are reduced by choosing $x\approx 1$, it will nevertheless be very difficult to interpret longitudinal response functions in terms of possible modifications of the one-body momentum distribution. A somewhat more promising approach might be to use R_T because the requirements of current conservation do not affect the transverse current directly. On the other hand, meson-exchange and isobar currents contribute primarily to the transverse response. The relative importance of those contributions tends to be reduced by using quasifree kinematics and can be reduced further by performing the experiment for large negative y, in other words, on the small-ω side of the quasifree peak. This conclusion is supported by the observation of y scaling in inclusive electron scattering for negative y and large q and has been used to deduce ground-state momentum densities [59]. Furthermore, the calculations of van der Sluys *et al.* [13] show that for fixed ω and p_m the relative importance of two-body currents decreases as q and, consequently, x increase. Therefore, we suggest that similar measurements for single-nucleon knockout should employ R_T for negative y and large q.

3. Recoil polarization

The dependence of the recoil polarization observables upon gauge is shown in Fig. 12 for proton knockout and in Fig. 13 for neutron knockout. The dependence upon gauge is minimal for the helicity-independent polarization P_y, which vanishes in the absence of final-state interactions—P_y depends primarily upon the optical potential and is practically independent of the current operator. For the helicity-dependent components P'_x and P'_z, the gauge dependence is quite small for $p_m\lesssim 250$ MeV/c and remains relatively small even for larger p_m. Similarly, recoil polarization observables calculated within the usual Coulomb gauge for the $\{\Gamma_{cc1},\Gamma_{cc2},\Gamma_{cc3}\}$ vertex functions are compared for proton knockout in Fig. 12 or for neutron knockout in Fig. 13. These figures show that P_y is insensitive to variations of the off-shell extrapolation and that the ambiguities in P'_x and P'_z remain quite small. Therefore, unlike cross sections, recoil polarization observables for quasifree kinematics are rather insensitive to variations among one-body current operators of the de Forest type.

In the one-photon-exchange approximation, the recoil nucleon polarization produced by a longitudinally polarized electron beam scattered through an angle θ by a free-nucleon target has two nonvanishing components of the form [60]

$$P'_L = G_M^2 \frac{2\tau(1+\tau)^{1/2}[1+(1+\tau)\tan^2(\theta/2)]^{1/2}\tan(\theta/2)}{G_E^2+[\tau+2\tau(1+\tau)\tan^2(\theta/2)]G_M^2}, \tag{37a}$$

$$P'_S = -G_E G_M \frac{2[\tau(1+\tau)]^{1/2}\tan(\theta/2)}{G_E^2+[\tau+2\tau(1+\tau)\tan^2(\theta/2)]G_M^2}, \tag{37b}$$

where $\tau=Q^2/4m^2$. Hence, the ratio

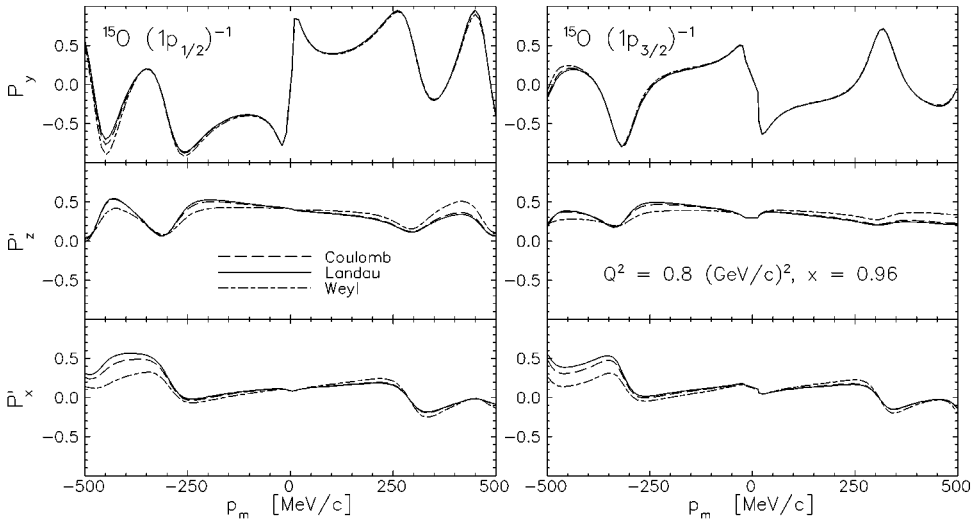

FIG. 13. DWIA calculations of recoil polarization for the $^{16}\mathrm{O}(\vec{e},e'\vec{n})$ reaction at the kinematics of TJNAF proposal No. 89-033 are shown using the cc1 current operator. Solid, dashed, and dot-dashed lines use the Landau, Coulomb, or Weyl gauges, respectively.

$$\frac{P'_S}{P'_L} = -\frac{G_E}{G_M}\left[\tau\left(1+(1+\tau)\tan^2\frac{\theta}{2}\right)\right]^{-1/2} \tag{38}$$

provides a means of measuring G_E/G_M that is relatively insensitive to systematic errors in the beam polarization and in the analyzing power of the polarimeter. It is important to recognize that for quasifree kinematics PWIA and DWIA calculations of the helicity-dependent recoil polarization produced by single-nucleon knockout from nuclei in quasifree kinematics with $p_m \lesssim 250$ MeV/c are quite similar, with optical model distortion producing only rather gentle modulations. Furthermore, both relativistic and nonrelativistic DWIA calculations also agree over this range of missing momentum. Nor do gauge or Gordon ambiguities affect these quantities for modest p_m. Therefore, to the extent that the one-body current operator dominates the knockout reaction, helicity-dependent recoil polarization provides a robust measure of the nucleon electromagnetic form factors in the nuclear environment.

Thus, TJNAF experiment 89-033 [16] is designed to measure possible medium modifications of the proton electromagnetic form factors. However, several calculations suggest that two-body currents affect the helicity-dependent recoil polarization [61,57]. It should be possible to investigate the roles of two-body currents and/or possible medium modifications of the one-body current using recoil polarization for modest p_m with relatively little uncertainty due to final-state interactions, gauge or Gordon ambiguities, or relativistic corrections.

IV. SUMMARY AND CONCLUSIONS

We have investigated some of the consequences of ambiguities in the one-body current operator for DWIA calculations of semiexclusive single-nucleon knockout over a wide range of kinematical conditions. These ambiguities can be classified in two categories: (1) gauge ambiguities arising from violation of current conservation by the off-shell vertex function and (2) Gordon ambiguities arising from transformations of the vertex function generated using the Gordon identity that are equivalent on shell but differ off shell. The present calculations were made using the nonrelativistic DWIA, but we also discuss the implications of stronger Gordon ambiguities encountered in calculations based upon the relativistic DWIA. Calculations for $^{16}\mathrm{O}(\vec{e},e'\vec{N})$ were presented for the kinematics of the Mainz measurements at small Q^2 and large missing momentum and for the kinematics of experiments at $Q^2=0.8$ (GeV/c)^2 in progress at TJNAF.

Although the p-shell $^{16}\mathrm{O}(e,e'p)$ data obtained at both NIKHEF and Mainz are in good agreement for $T_p \sim 100$ MeV, the cross sections obtained at Mainz near the peak of the momentum distribution using $T_p \sim 215$ MeV are factors of 0.5–0.6 smaller than predicted by DWIA calculations based upon spectroscopic factors and overlap functions fitted to the lower-energy data, which are consistent with systematics previously established for a broad range of nuclei. This discrepancy cannot be explained by reasonable variations of the optical model or the one-body current operator. Furthermore, the kinematics for small p_m are close enough to quasifree that one does not expect two-body currents to substantially reduce the cross section at the peak of the single-nucleon momentum distribution. Therefore, if the data of Blomqvist *et al.* [17] for $T_p \sim 215$ MeV are normalized correctly, there may be a serious error in the DWIA, whose origin is not understood, even when the kinematics are nearly quasifree. It is important to confirm these data and to extend the range of ejectile energy upwards.

We find that Gordon ambiguities in nonrelativistic DWIA calculations of the differential cross section are unimportant for small Q^2 but approach 35% for $p_m \sim 500$ MeV/c and $Q^2=0.8$ (GeV/c)^2. However, Udías *et al.* [14] find that Gordon ambiguities are about 10% for small p_m and approach an order of magnitude for $p_m \sim 500$ MeV/c and $Q^2 \sim 0.04$ (GeV/c)^2. Conversely, we find that gauge ambiguities in nonrelativistic DWIA cross sections approach an order of magnitude for $p_m \sim 500$ MeV/c and $Q^2 \sim 0.04$ and remain important, but are somewhat smaller, for $Q^2 \sim 0.8$ (GeV/c)^2. For large p_m, gauge ambiguities are

smaller for quasifree kinematics ($x \approx 1$) than for the small-x experiments performed at low Q^2. These ambiguities in the one-body current operator are as large or larger than the modifications of the missing momentum distributions for valence knockout that are expected from both long-range and short-range correlations. Furthermore, channel coupling in final-state interactions and contributions from two-body currents also become quite important for large missing momentum. Therefore, we conclude that it will not be possible to extract information about correlations from valence single-nucleon knockout by electron scattering before considerable progress is made in understanding the one-body and two-body current operators. Further investigation is needed to evaluate ambiguities in the current operator and final-state interactions for knockout reactions that probe the continuum at large p_m and E_m where short-range correlations become most prominent.

Gauge ambiguities in the longitudinal response function R_L increase with p_m, while for the longitudinal-transverse interference response function R_{LT} gauge ambiguities vary more slowly and remain important even for small p_m. Furthermore, Gordon ambiguities in the azimuthal asymmetry, A_ϕ, are quite small for nonrelativistic DWIA. Therefore, A_ϕ may provide a useful means for selecting a gauge using experimental data.

The helicity-independent polarization depends upon final-state interactions and is rather insensitive to the current operator. The helicity-dependent polarization $\mathbf{P}'$ is sensitive to the nucleon electromagnetic form factors and to the spin structure of the vertex function. For $p_m \lesssim 250$ MeV/c, $\mathbf{P}'$ appears to be quite insensitive to final-state interactions. With different spin structure, two-body currents can produce appreciable effects upon $\mathbf{P}'$. In contrast to the differential cross section and unpolarized response functions, recoil polarization observables are much less sensitive to gauge and Gordon ambiguities. Therefore, measurements of the helicity-dependent recoil polarization for modest p_m provide sensitivity to possible medium modifications of the nucleon form factors or to two-body currents.

The nature of the off-shell single-nucleon electromagnetic vertex function in the nuclear medium remains the most important unsolved theoretical problem in electronuclear physics. We have investigated some of the consequences of uncertainties in this operator upon the interpretation of several experiments of current interest, but unfortunately there exists no compelling theoretical argument for selecting a preferred form or gauge. Until a more fundamental theory is developed, which is beyond the scope of the present work, one might as well continue to employ the traditional choices of the de Forest cc1 current and the Coulomb gauge but should be aware of the interpretative limitations incurred by these more or less arbitrary choices.

ACKNOWLEDGMENTS

The support of the U.S. National Science Foundation under Grant No. PHY-9513924 is gratefully acknowledged.

[1] J. J. Kelly, Adv. Nucl. Phys. **23**, 75 (1996).
[2] S. Boffi, C. Giusti, and F. D. Pacati, Phys. Rep. **226**, 1 (1993).
[3] S. Boffi, C. Giusti, F. D. Pacati, and M. Radici, *Electromagnetic Response of Atomic Nuclei* (Oxford University Press, Oxford, 1996).
[4] A. E. L. Dieperink and P. K. A. de Witt Huberts, Annu. Rev. Nucl. Part. Sci. **40**, 239 (1990).
[5] S. Frullani and J. Mougey, in *Advances in Nuclear Physics*, edited by J. W. Negele and E. Vogt (Plenum Press, New York, 1984), Vol. 14.
[6] A. Polls, M. Radici, S. Boffi, W. H. Dickhoff, and H. Müther, Phys. Rev. C **55**, 810 (1997).
[7] Z. Y. Ma and J. Wambach, Nucl. Phys. **A402**, 275 (1983).
[8] Z. Y. Ma and J. Wambach, Phys. Lett. B **256**, 1 (1991).
[9] C. Mahaux and H. Ngô, Nucl. Phys. **A431**, 486 (1984).
[10] C. Mahaux and R. Sartor, Nucl. Phys. **A503**, 525 (1989).
[11] C. Mahaux and R. Sartor, Adv. Nucl. Phys. **20**, 1 (1991).
[12] I. Bobeldijk *et al.*, Phys. Rev. Lett. **73**, 2684 (1994).
[13] V. van der Sluys, J. Ryckebusch, and M. Waroquier, Phys. Rev. C **54**, 1322 (1996).
[14] J. M. Udías, P. Sarriguren, E. M. de Guerra, and J. A. Caballero, Phys. Rev. C **53**, R1488 (1996).
[15] A. Saha *et al.*, ''Study of the Quasielastic $(e,e'p)$ Reaction in ^{16}O at High Recoil Momentum,'' TJNAF Proposal No. 89-003, 1989.
[16] C. Glashausser *et al.*, ''Measurement of Recoil Polarization in the ^{16}O$(e,e'p)$ Reaction with 4 GeV Electrons,'' TJNAF Proposal No. 89-033, 1989.
[17] K. I. Blomqvist *et al.*, Phys. Lett. B **344**, 85 (1995).
[18] T. de Forest, Nucl. Phys. **A392**, 232 (1983).
[19] A. Picklesimer, J. W. van Orden, and S. J. Wallace, Phys. Rev. C **32**, 1312 (1985).
[20] H. W. L. Naus, S. J. Pollock, J. H. Koch, and U. Oelfke, Nucl. Phys. **A509**, 717 (1990).
[21] S. Pollock, H. W. L. Naus, and J. H. Koch, Phys. Rev. C **53**, 2304 (1996).
[22] C. R. Chinn and A. Picklesimer, Nuovo Cimento A **105**, 1149 (1992).
[23] J. Ryckebusch, K. Heyde, D. van Neck, and M. Waroquier, Nucl. Phys. **A503**, 694 (1989).
[24] J. Ryckebusch, M. Waroquier, K. Heyde, J. Moreau, and D. Ryckbosch, Nucl. Phys. **A476**, 237 (1988).
[25] V. Devanathan, Ann. Phys. (N.Y.) **43**, 74 (1967).
[26] N. Dombey, Rev. Mod. Phys. **41**, 236 (1969).
[27] T. de Forest, Ann. Phys. (N.Y.) **45**, 365 (1967).
[28] J. Mougey, M. Bernheim, A. Bussière, A. Gillebert, P. X. Hô, M. Priou, D. Royer, I. Sick, and G. Wagner, Nucl. Phys. **A262**, 461 (1976).
[29] R. G. Sachs, Phys. Rev. **126**, 2256 (1962).
[30] W. Gordon, Z. Phys. **50**, 630 (1928).
[31] J. D. Bjorken and S. D. Drell, *Relativistic Quantum Mechanics* (McGraw-Hill, New York, 1964).
[32] S. Boffi, C. Giusti, F. D. Pacati, and S. Frullani, Nucl. Phys. **A319**, 461 (1979).
[33] Y. Jin, H. P. Blok, and L. Lapikás, Phys. Rev. C **48**, R964 (1993).

[34] L. L. Schiff, Phys. Rev. **103**, 443 (1956).
[35] J. M. Udías, P. Sarriguren, E. M. de Guerra, E. Garrido, and J. A. Caballero, Phys. Rev. C **48**, 2731 (1993).
[36] M. F. Gari and W. Krümpelmann, Phys. Lett. B **274**, 159 (1992).
[37] M. F. Gari and W. Krümpelmann, Phys. Lett. B **282**, 483 (1992).
[38] F. Perey and B. Buck, Nucl. Phys. **32**, 353 (1962).
[39] F. G. Perey, in *Direct Interactions and Nuclear Reaction Mechanisms*, edited by E. Clementel and C. Villi (Gordon Breach, New York, 1963), pp. 125–138.
[40] E. N. M. Quint, Ph.D. thesis, Universiteit van Amsterdam, 1988.
[41] M. Zhongyu and F. Dachun, Phys. Rev. C **45**, 811 (1992).
[42] M. Leuschner *et al.*, Phys. Rev. C **49**, 955 (1994).
[43] C. Giusti and F. D. Pacati, Nucl. Phys. **A504**, 685 (1989).
[44] A. Picklesimer and J. W. van Orden, Phys. Rev. C **40**, 290 (1989).
[45] V. Dmitrasinovic, Phys. Rev. C **47**, 2195 (1993).
[46] E. D. Cooper, S. Hama, B. C. Clark, and R. L. Mercer, Phys. Rev. C **47**, 297 (1993).
[47] P. Schwandt, H. O. Meyer, W. W. Jacobs, A. D. Bacher, S. E. Vigdor, M. D. Kaitchuck, and T. R. Donoghue, Phys. Rev. C **26**, 55 (1982).
[48] H. Seifert *et al.*, Phys. Rev. C **47**, 1615 (1993).
[49] J. J. Kelly, Phys. Rev. C **54**, 2547 (1996).
[50] D. G. Madland, Technical Report No. LA-UR-97-0306, Los Alamos National Laboratory, 1997 (unpublished).
[51] M. Hedayati-Poor, J. I. Johansson, and H. S. Sherif, Phys. Rev. C **51**, 2044 (1995).
[52] S. Boffi and M. Radici, Phys. Lett. B **242**, 151 (1990).
[53] Y. Jin, D. S. Onley, and L. E. Wright, Phys. Rev. C **50**, 168 (1994).
[54] C. M. Spaltro, H. P. Blok, E. Jans, L. Lapikás, M. van der Schaar, G. van der Steenhoven, and P. K. A. de Witt Huberts, Phys. Rev. C **48**, 2385 (1993).
[55] L. Chinitz *et al.*, Phys. Rev. Lett. **67**, 568 (1991).
[56] S. Boffi and M. Radici, Nucl. Phys. **A526**, 602 (1991).
[57] S. Boffi, M. Radici, J. J. Kelly, and T. M. Payerle, Nucl. Phys. **A539**, 597 (1992).
[58] V. van der Sluys, J. Ryckebusch, and M. Waroquier, Phys. Rev. C **49**, 2695 (1994).
[59] D. B. Day, J. S. McCarthy, T. W. Donnelly, and I. Sick, Annu. Rev. Nucl. Part. Sci. **40**, 357 (1990).
[60] R. G. Arnold, C. E. Carlson, and F. Gross, Phys. Rev. C **23**, 363 (1981).
[61] S. Boffi, C. Giusti, F. D. Pacati, and M. Radici, Nucl. Phys. **A518**, 639 (1990).